Descriptive study of the even-even actinide nuclei $^{230-234}$Th isotopes using IBM-1

N. Al-Dahan[1)]

Department of Physics, College of Science, University of Kerbala, 56001 Kerbala, Iraq

Abstract: The nuclear structure of the actinide even–even thorium isotopes from A=230-234 have been investigated within the framework of the Interacting Boson Model (IBM-1). Predictions are given for the excited state energies for the ground state, β and γ-bands, the transition probabilities between these states, the rotational moment of inertia, and the energy staggering in the γ-band energies. The results of these calculations are compared with the experimental data on these isotopes.

Keywords: IBM, energy levels, B(E2) values, staggering in γ-band energies, potential energy surface

PACS: 21.60.Ev, 27.70.+q, 23.20.-g **DOI:** 10.1088/1674-1137/41/6/064105

1 Introduction

The atomic nucleus is a many-body, strongly formed interaction quantal system. The coherence of many possible basis wave functions between different single-particle configurations can lead to collective properties in many nuclei, which exhibit themselves in a range of deformed shapes for the nuclear mean field [1]. A strongly prolate or oblate deformed nucleus can rotate and exhibit the characteristic $I(I+1)$ rotational band structure in its intrinsic energy spacing, sometimes with remarkable regularity [1–4].

The properties of excited nuclear states, such as excitation energy, spin and parity, and electromagnetic transitions probabilities, are determined by the intrinsic, underlying shape or deformation of the nuclear mean field and its (proton) charge distribution [5]. It is particularly important to analyse the structure of heavy actinide nuclei where the quadrupole deformation is well established and noted [6–10].

The Interacting Boson Model (IBM-1) [4, 11] has been found to be successful in phenomenological studies when describing the low-lying levels and quadrupole collective states of medium and heavy nuclei. The microscopic foundation of the IBM has been studied extensively in order to derive an IBM Hamiltonian starting from the underlying nucleon degrees of freedom [12–15].

It is known that IBM expects very strong odd-even energy staggering (OES) in $U(5)$ and $O(6)$ limits, while in the exact $SU(3)$ limit there is no staggering in the gamma band energies. Very small staggering can be induced by band mixing with the ground and the excited $K = 0$ band. Well deformed nuclei that show sizeable staggering deviate from $SU(3)$ in the direction of either $U(5)$ or $O(6)$, which exhibit large staggering. The OES in the $K = 2$, gamma band has been interpreted as a result of the interaction between the even angular momentum of the γ band and the corresponding states in the β band [16]. This suggestion has been addressed to the $SU(3)$ limit in which the lowest β and γ rotational bands interact in the framework of the same irreducible representation (λ, μ=2) of the group $SU(3)$ [15–18].

The $SU(3)$ geometrical limit describes a particular kind of deformed rotational nucleus, which shows a low lying $K^\pi = 2^+$and $K^\pi = 0^+$ excited state bandheads, usually referred to as the γ and β band, respectively. Excitation modes built on these bandheads can result in even-spin states which are near-degenerate. In the $SU(3)$ limit, transitions from the γ band to the ground band are forbidden. Empirically, these bands seldom degenerate exactly. Furthermore, γ to ground band B(E2) values are known to be collective (typically 5–10W.u.) [6]. These two features rule out an exact $SU(3)$ description of these nuclei and, indeed, most collective model descriptions of such deformed nuclei have used broken-$SU(3)$ numerical diagonalizations of the IBM Hamiltonian [6]. A recent survey of well-deformed rare earth nuclei showed that $B(E2)$ values from the γ band to the ground band could be approximately explained by a parameter-free description in terms of a partial dynamical symmetry (PDS) [6]. A description of the collective states of the ground state, β- and γ-bands and an analysis of the spectrum of lanthanide and actinide neighbour even–even nuclei are important [19].

Received 11 January 2017, Revised 4 March 2017

1) E-mail: nawrasaldahan@uokerbala.edu.iq

A few studies have been conducted on the structure of the thorium nucleus in recent years. In 2013, K. Nomura et al. studied the shape phase transition [20] between stable octupole deformation and octupole vibrations in thorium nuclei, using a microscopic framework based on nuclear density functional theory for the analysis [20]. In the same year (2013) Li et al. studied the collective Hamiltonian description of the octupole shape phase transition for the Th isotopes [21]. For two regions of octupole deformation and collectivity – Th, Ra, Sm, and Ba-K. Nomura et al. [22] used the IBM Hamiltonian to calculate excitation spectra and transition rates for the positive- and negative-parity collective states in four isotopic chains. Due to the lack of experimental information on Th isotopes in this part of the nuclear chart, more theoretical calculations are needed to clarify the underlying structure of these isotopes.

The aim of this work is to study the nuclear structure of the deformed even-even thorium ($A=230-234$) isotopes using the IBM-1 prescription.

2 Theoretical background

2.1 Interacting boson model (IBM-1)

The IBM-1 model of Arima and Iachello [23, 24] has become widely accepted as a workable theoretical scheme for describing the low-lying collective properties of nuclei across an entire major shell using a simple Hamiltonian [25]. In the IBM, the properties of a low-lying collective for even-even nuclei are described in terms of the interacting s bosons (L=0) and d bosons (L=2) [23, 26]. The valence particles outside the major closed shells dominate and are thus studied as a part of the structure of the low-lying levels. The numbersN_π and N_v are proton bosons and neutron bosons, respectively. These are counted from the nearest closed shell, with the total boson number defined as $N=N_\pi+N_v$. This model, and the underlying structure of the six-dimensional unitary group $SU(6)$, leads to a simple Hamiltonian capable of describing three dynamical symmetries, namely $U(5)$ corresponding to a vibrational limit [24], $SU(3)$ corresponding to an axially symmetric rotationally limit [27] and $O(6)$ which corresponds to a γ-unstable rotational limit [28]. Furthermore, there is also the presence of transitional nuclei [29]. It is intermediate between these limits.

The most general parameterization of the IBM-1 Hamiltonian can be written in the following multipole form [4, 25]

$$\hat{H}=\varepsilon\hat{n}_d+a_0\left(\hat{P}^\dagger.\hat{P}\right)+a_1\left(\hat{L}.\hat{L}\right)+a_2\left(\hat{Q}.\hat{Q}\right)+a_3 +\left(\hat{T}_3.\hat{T}_3\right)+a_4\left(\hat{T}_4.\hat{T}_4\right) \quad (1)$$

where $\hat{n}_d=(\hat{d}^\dagger.\hat{\tilde{d}})$is the d-boson number operator, $\hat{P}=1/2(\hat{\tilde{d}}.\hat{\tilde{d}})-1/2(\hat{\tilde{s}}.\hat{\tilde{s}})$is used to show the pairing boson operator,$\hat{L}=\sqrt{10}[\hat{d}^\dagger\times\hat{\tilde{d}}]^{(1)}$ gives the angular momentum operator, $\hat{T}_3=[\hat{d}^\dagger\times\hat{\tilde{d}}]^{(3)}$ is the octupole operator, $\hat{T}_4=[\hat{d}^\dagger\times\hat{\tilde{d}}]^{(4)}$ is the hexadecapole operator, $\hat{Q}=[(\hat{d}^\dagger\times\hat{\tilde{s}})+(\hat{\tilde{s}}^\dagger\times\hat{\tilde{d}})]^{(2)}-\frac{\sqrt{7}}{2}[\hat{d}^\dagger\times\hat{\tilde{d}}]^{(2)}$ represents the quadrupole operator, $\varepsilon=\varepsilon_d-\varepsilon_s$ is the boson energy, and a_0,a_1,a_2,a_3, and, a_4 are the phenomenological parameters. The $\hat{Q}$ operator is used to calculate electromagnetic transition strengths and moments T(E2)= $e_{\rm B}\hat{Q}$[29,30] , where e_B is the boson effective charge.

Two Hamiltonians of IBM-1 [4, 25] were used in the present work, as follows:

$$\hat{H}=a_1(\hat{L}.\hat{L})+a_2(\hat{Q}.\hat{Q}) \quad (2)$$

and

$$\hat{H}=\varepsilon\hat{n}_d+a_1\left(\hat{L}.\hat{L}\right)+a_2\left(\hat{Q}.\hat{Q}\right) \quad (3)$$

where a_0= 2PAIR, a_1= 1/2 ELL, a_2= 1/2 QQ, ε= EPS.

2.2 Reduced transition probabilities, B(E2)

The general form of the B(E2) operator in IBM-1 is given as follows [23, 26, 32–34]:

$$\widehat{T}_\mu^{(E2)}=\alpha_2[\widehat{d}^\dagger\times\widehat{\tilde{s}}+\widehat{s}^\dagger\times\widehat{\tilde{d}}]_\mu^{(2)}+\beta_2[\widehat{d}^\dagger\times\tilde{d}]_\mu^{(2)} \quad (4)$$

The reduced E2 transition probability (E2) is illustrated as [8, 9]:

$$B(\mathrm{E2};I_i\to I_f)=\frac{1}{(2I_i+1)}\left|\left\langle I_f\left\|T^{(\mathrm{E2})}\right\|I_i\right\rangle\right|^2 \quad (5)$$

The general form to calculate the relative B(E2) values of transition for γ -bands is shown as [35]:

$$B\,(\mathrm{E2})=100\left(\frac{I_\gamma}{I_\gamma^{\mathrm{ref}}}\right)\left(\frac{E_\gamma^{\mathrm{ref}}}{E_\gamma}\right)\left(\frac{1+\frac{1}{\delta^2_{\mathrm{ref}}}}{1+\frac{1}{\delta^2}}\right), \quad (6)$$

where I_γ is the intensity of the transition, E_γ is the gamma ray energy, δ is the mixing ratio and ref stands for the reference transition.

2.3 Moment of inertia and square of rotational energy

The general form for calculating the moment of inertia $\frac{2\vartheta}{\hbar^2}$ and the square of the rotational energy $(\hbar\omega)^2$ are [36, 37]

$$\frac{2\vartheta}{\hbar^2}=\frac{4L-2}{E(L)-E(L-2)}=\frac{4L-2}{E_\gamma}(\mathrm{MeV})^{-1} \quad (7)$$

$$\text{and } (\hbar\omega)^2=\left[\frac{E(L)-E(L-2)}{\sqrt{L(L+1)}-\sqrt{(L-2)(L-1)}}\right]^2 (\text{MeV})^2 \quad (8)$$

where ϑ is the moment of inertia, E_γ is the transition energy, and the L is angular momentum of the initial, decaying state [37].

2.4 Staggering in γ-band energies

The symmetry changes $SU(3)$, $U(5)$ and $O(6)$ information carried by the OES effect is observed in the γ–bands; this is among the most sensitive phenomena noted [38]. It is most strongly pronounced in nuclei characterized by the $U(5)$ and $O(6)$ limits and it is relatively weaker in nuclei close to $SU(3)$ symmetry [38]. In even-even nuclei, the odd-even staggering represents a relative displacement of the odd-angular momentum levels for the γ band with respect to their neighbouring states, even where this includes angular momentum [17]. The staggering between in γ-band energies is defined by [39, 40]:

$$S(J) = \frac{\left\{E\left(J_\gamma^+\right)-E\left[(J-1)_\gamma^+\right]\right\}-\left\{E\left[(J-1)_\gamma^+\right]-\left[(J-2)_\gamma^+\right]\right\}}{E\left(2_1^+\right)} \quad (9)$$

2.5 Potential energy surface

The potential energy surface, in general, as a function of geometrical variables β and γ is given by [25]:

$$E(N,\beta,\gamma)=\frac{N\varepsilon_d\beta^2}{(1+\beta^2)}+\frac{N(N-1)}{(1+\beta^2)^2}(\alpha_1\beta^4+\alpha_2\beta^3\cos 3\gamma+\alpha_3\beta^2+\alpha_4), \quad (10)$$

where N is the total boson number, ε_d is the d boson energy, β is the quadrupole deformation parameter, γ is the asymmetry angle, taking values from 0° to 60°, and $\alpha_1,\alpha_2,\alpha_3$, and α_4 are parameters of the potential surface.

3 Results and discussion

In the current work, the predicted energy levels, reduced electric quadrupole transition probabilities, staggering in γ-band energies, overlap with $SU(3)$ limit of the wave function, and potential energy surfaces for ^{230,232,234}Th isotopes have been investigated using two different procedures, and subsequently compared with the experimental data:

(a) (Th.) using Hamiltonian equation (2)

(b) (Th. +EPS) using Hamiltonian equation (3) using the IBM-1code PHINT [41].

3.1 Energy levels

In the present study, the rotational limit of the IBM-1 has been used to calculate energy levels for $^{230-234}$Th isotopes and the breaking of this limit by the introduction of the EPS term (ε) into the Hamiltonian equation. The excitation energy ratios $E(4_1^+)/E(2_1^+)=R(4/2)$ for ^{230,232,234}Th are 3.27, 3.28 and 3.29, respectively [42]. This near-ideal rotor value reflects the emergence of nuclear quadrupole collectivity, which can be used to distinguish between the $U(5)$, $SU(3)$ and $O(6)$ limits of the IBM [43]. The first 2^+ state ($E(2_1^+)$) of ^{230,232,234}Th decreases smoothly with increasing mass number, indicating that these Th isotopes are close to the $SU(3)$ limit. Two sets of parameters for Th isotopes which were applied in the current work are shown in Tables 1 and 2. The parameters for EPS, ELL and Q.Q were changed by values typical of the expected changes from one nucleus to its neighboring region. The Q.Q parameter for ^{234}Th was estimated by calculating the energy of the second 2^+ state from the expressions [39]:

$$E_{\text{rot}}(J)=\frac{\hbar^2}{2I}[J(J+1)-K(K+1)] \quad (11)$$

Table 1. Adopted values for the parameters used for IBM-1 calculations using Hamiltonian equation for $SU(3)$ limit, where N = boson number, EPS = energy, PAIR = pairing, ELL = angular momentum, QQ = quadrupole, OCT = octupole, HEXA = hexadecapole, and CHI= $\sqrt{5}\chi$). All the parameters are in MeV except CHI.

isotopes	N	EPS	PAIR	ELL	QQ	OCT	HEXA	CHI
^{230}Th	11	0.0	0.000	0.0130	−0.0198	0.0	0.0	−2.958
^{232}Th	12	0.0	0.000	0.0084	−0.0214	0.0	0.0	−2.958
^{234}Th	13	0.0	0.000	0.0082	−0.0216	0.0	0.0	−2.958

Table 2. Adopted values for the parameters used for IBM-1 calculations using Hamiltonian equation for $SU(3)$ limit + eps, all parameters in MeV except CHI.

isotopes	N	EPS	PAIR	ELL	QQ	OCT	HEXA	CHI
^{230}Th	11	0.0530	0.000	0.0090	−0.0208	0.0	0.0	−2.958
^{232}Th	12	0.0493	0.000	0.0073	−0.0217	0.0	0.0	−2.958
^{234}Th	13	0.0490	0.000	0.0074	−0.0219	0.0	0.0	−2.958

The calculated energy levels were compared with the available experimental values as shown in Figs. 1–3. These calculations give a reasonable description of the energy systematic of the low-lying states. Additional levels were predicted by these IBM calculations which have not yet been observed experimentally. The comparison illustrates that an effective agreement is found between the experimental and the calculated values. Generally, the ground bands and beta bands in all their isotopes are well reproduced. The gamma-band states in the second procedure (as shown in Section 3(b)) for the ^{230}Th isotope are in reasonable agreement with the experimental data. As shown in Figs. 2 and 3, for each band the level energies follow closely the expected $L(L+1)$ behavior expected for rotational nuclei. The beta and gamma bands have similar excitation energies, suggesting that the ^{232,234}Th isotopes are approaching the SU(3) limit.

3.2 B(E2) values

The transition probabilities and related B(E2) values were calculated. The values of E2SD (E2SD=α_2), and E2DD (E2DD=$\sqrt{5}\beta_2$) [31] have been selected to be compatible with the $SU(3)$ limit. The values of E2SD were determined by normalizing the calculations to the previously experimentally determined$B(\mathrm{E2}: 2_1^+ \to 0_1^+)$values. The parameter values of E2DD and E2SD are summarized in Table 3. The calculated values of B(E2) for the isotopes under study, together with the available experimental values [42], are shown in Table 4. The B(E2) values for the$(2_1^+ \to 0_1^+), (4_1^+ \to 2_1^+)$decay decreases with increasing mass number, A. The transitions

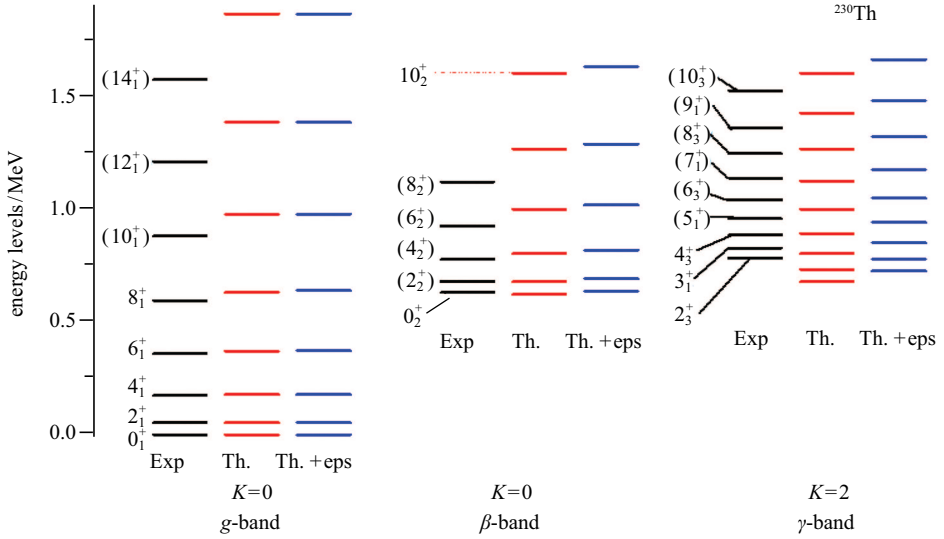

Fig. 1. (color online) The calculated low-lying energy levels using IBM-1 and the experimental data [42] of ^{230}Th isotope.

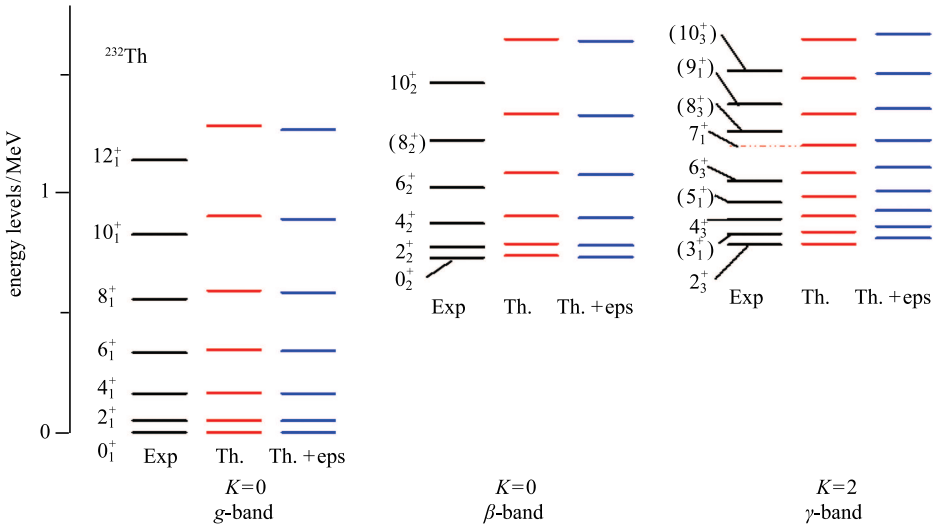

Fig. 2. (color online) The calculated low-lying energy levels using IBM-1 and the experimental data [42] of ^{232}Th isotope.

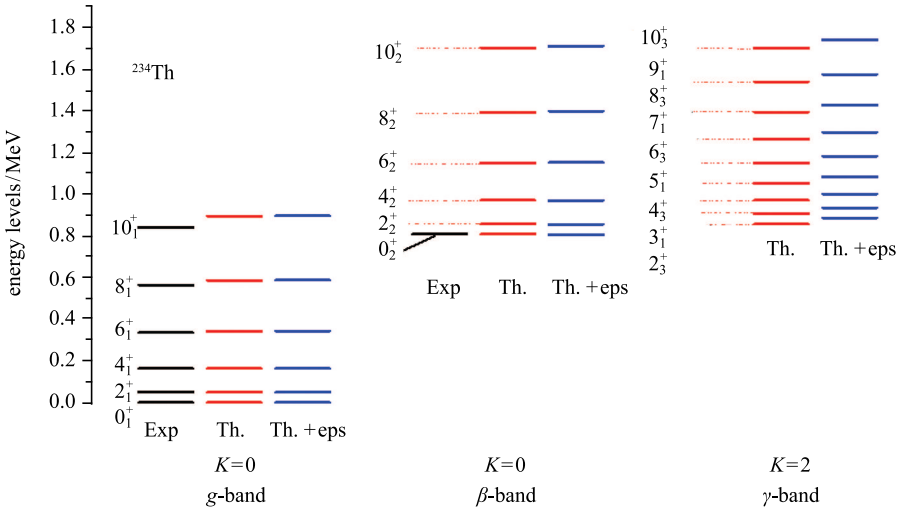

Fig. 3. (color online) The calculated low-lying energy levels using IBM-1 and the experimental data [42] of ^{234}Th isotope.

$(2_2^+ \to 2_1^+), (4_2^+ \to 4_1^+), (3_1^+ \to 4_1^+)$ are forbidden in the $SU(3)$ limit [4] and are rather weak, as expected, as can be seen in Tables 4 and 5. Overall, the calculated results are in agreement with experimental values. The calculated wave functions can be further tested using the $B(E2)$ values. The overlaps of the wave functions for the $SU(3)$ symmetry are 1. To calculate the overlap of any isotope, one has to calculate the wave functions of this isotope. Therefore, in such a study the wave functions of ^{230,232,234}Th isotopes were calculated. The overlap is obtained by taking the sum of the multiplications of the corresponding terms of the wave functions of each state in these isotopes. However, the calculated overlaps come to 1 for ^{230,232,234}Th isotopes in applying the Hamiltonian equations without EPS; they run approximately to 0.99 when the Hamiltonian equation with EPS is applied, as shown in Table 6, which shows the overlaps for the first $0_1^+ 2_1^+$, 4_1^+ and 2_2^+ states of ^{230,232,234}Th isotopes.

Table 3. The values of parameters E2SD and E2DD in (e^2b^2) of B(E2) for ^{230,232,234}Th isotopes.

isotopes	E2SD	E2DD
^{230}Th	1	−1.2108
^{232}Th	1	−1.0556
^{234}Th	1	−1.9556

Table 4. B(E2) values for ^{230,232,234}Th isotopes in (e^2b^2)

isotopes	$J_i \to J_f$	EXP B(E2)[42]	Th. B(E2)	Th. + eps B(E2)
^{230}Th	$2_1^+ \to 0_1^+$	1.640	1.640	1.644
	$4_1^+ \to 2_1^+$	2.218	2.300	2.306
	$6_1^+ \to 4_1^+$	—	2.449	2.455
	$2_2^+ \to 0_1^+$	0.022	0.027	0.001
	$2_2^+ \to 2_1^+$	–	0.021	0.002
	$2_2^+ \to 4_1^+$	0.083	0.009	0.005
	$4_2^+ \to 4_1^+$	—	0.043	0.001
	$4_2^+ \to 6_1^+$	—	0.008	0.006
	$3_1^+ \to 2_1^+$	—	0.042	0.051
	$3_1^+ \to 4_1^+$	—	0.022	0.028
	$2_3^+ \to 0_1^+$	0.024	0.001	0.029
	$2_3^+ \to 2_1^+$	0.046	0.023	0.048
	$2_3^+ \to 4_1^+$	0.003	0.007	0.003
	$4_3^+ \to 2_1^+$	—	0.003	0.013
	$4_3^+ \to 6_1^+$	—	0.013	0.007

Continued

isotopes	$J_i \to J_f$	EXP B(E2)[42]	Th. B(E2)	Th. + eps B(E2)
^{232}Th	$2_1^+ \to 0_1^+$	1.676	1.676	1.677
	$4_1^+ \to 2_1^+$	2.421	2.357	2.358
	$6_1^+ \to 4_1^+$	2.760	2.525	2.524
	$2_2^+ \to 0_1^+$	0.023	0.013	0.002
	$2_2^+ \to 2_1^+$	0.004	0.0001	0.003
	$2_2^+ \to 4_1^+$	0.027	0.019	0.008
	$3_1^+ \to 2_1^+$	—	0.049	0.056
	$3_1^+ \to 4_1^+$	—	0.026	0.030
	$3_1^+ \to 4_1^+$	0.0001	0.015	0.003
	$4_2^+ \to 6_1^+$	—	0.008	0.009
	$2_3^+ \to 0_1^+$	0.024	0.019	0.032
	$2_3^+ \to 2_1^+$	0.061	0.052	0.052
	$2_3^+ \to 4_1^+$	0.001	0.0001	0.003
	$4_3^+ \to 2_1^+$	0.0001	0.004	0.015
	$4_3^+ \to 6_1^+$	0.0002	0.015	0.007
^{234}Th	$2_1^+ \to 0_1^+$	1.569	1.569	1.564
	$4_1^+ \to 2_1^+$	—	2.211	2.205
	$6_1^+ \to 4_1^+$	—	2.376	2.369
	$2_2^+ \to 0_1^+$	—	0.005	0.005
	$2_2^+ \to 2_1^+$	—	0.007	0.007
	$2_2^+ \to 4_1^+$	—	0.001	0.0009
	$3_1^+ \to 2_1^+$	—	0.009	0.009
	$3_1^+ \to 4_1^+$	—	0.004	0.004
	$4_2^+ \to 2_1^+$	—	0.003	0.003
	$4_2^+ \to 6_1^+$	—	0.004	0.004
	$2_3^+ \to 0_1^+$	—	0.0003	0.0003
	$2_3^+ \to 2_1^+$	—	0.002	0.002
	$2_3^+ \to 4_1^+$	—	0.002	0.002
	$4_3^+ \to 2_1^+$	—	0.0003	0.0002
	$4_3^+ \to 2_1^+$	—	0.009	0.009
	$2_3^+ \to 0_1^+$	—	0.00008	0.00008

Table 5. B(E2) values for ^{230,232,234}Th isotopes.

isotopes	B(E2)ratio	EXP[42]	Th.	Th. + EPS
^{230}Th	$\frac{4_1^+ \to 2_1^+}{2_1^+ \to 0_1^+}$	1.352	1.402	1.402
	$\frac{2_2^+ \to 2_1^+}{2_1^+ \to 0_1^+}$	—	0.012	0.001
^{232}Th	$\frac{4_1^+ \to 2_1^+}{2_1^+ \to 0_1^+}$	1.444	1.406	1.406
	$\frac{2_2^+ \to 2_1^+}{2_1^+ \to 0_1^+}$	0.002	0.00005	0.002
^{234}Th	$\frac{4_1^+ \to 2_1^+}{2_1^+ \to 0_1^+}$	—	1.409	1.409
	$\frac{2_2^+ \to 2_1^+}{2_1^+ \to 0_1^+}$	—	0.004	0.004

Table 6. The overlap for the first $0_1^+, 2_1^+, 4_1^+$ and 2_2^+ states of ^{230,232,234}Th isotopes, the calculated wave functions were provided using the Hamiltonian equation with EPS.

isotopes(Th.+eps)	0_1^+	2_1^+	4_1^+	2_2^+
^{230}Th	0.99075	0.990967	0.991425	0.983356
^{232}Th	0.99344	0.993551	0.993827	0.98612
^{234}Th	0.99427	0.994354	0.994558	0.979914

The relative B(E2) values of the inter-band transition from $2_\gamma^+, 4_\gamma^+, 3_\gamma^+$, and 5_γ^+ states to ground states for ^{230,232,234}Th were calculated and were compared with the experimental data, as shown in Figs. 4, 5 and 6, and good agreement was found.

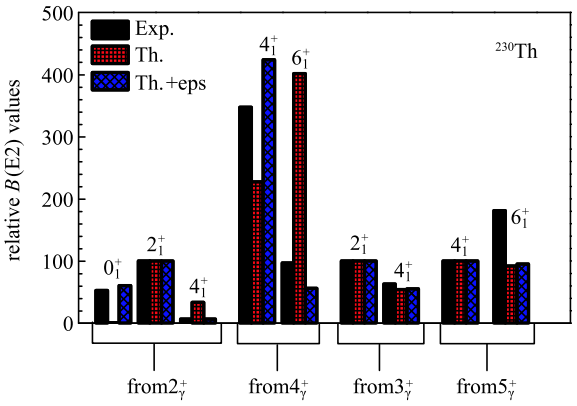

Fig. 4. (color online) The calculated and experimental values [42] of relative B(E2) for ^{230}Th isotope.

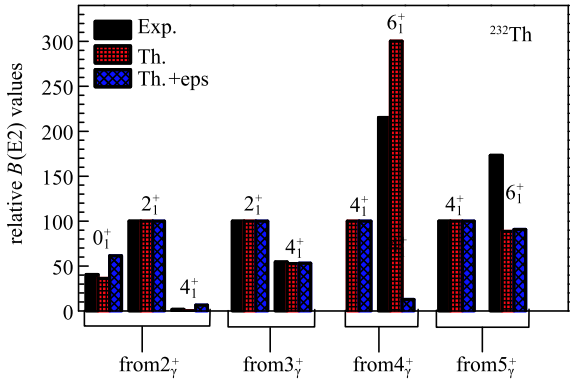

Fig. 5. (color online) The calculated and experimental values [42] of relative B(E2) for ^{232}Th isotope.

3.3 Moment of inertia and square of rotational energy

The moment of inertia and the square of rotational energy for the ground state band of even-even $^{230-234}$Th isotopes has been calculated, as shown in Figs. 7, 8 and 9. The ^{232}Th isotope shows a backbending effect at $I = 18^+$, which means there is a band crossing. It then changes behavior and increases gradually. This occurs in some heavy nuclei because the rotational energy increases, so the energy required to break a pair of coupled nucleons increases. In this effect, the unpaired nucleons move into different orbits and change the nuclear moment of inertia [36]. The ^{230,234}Th isotopes no longer have backbending, which that means the properties of these isotopes run unchanged.

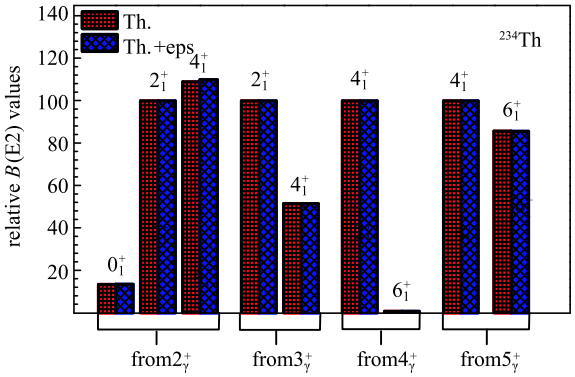

Fig. 6. (color online) The calculated values of relative B(E2) for ^{234}Th isotope.

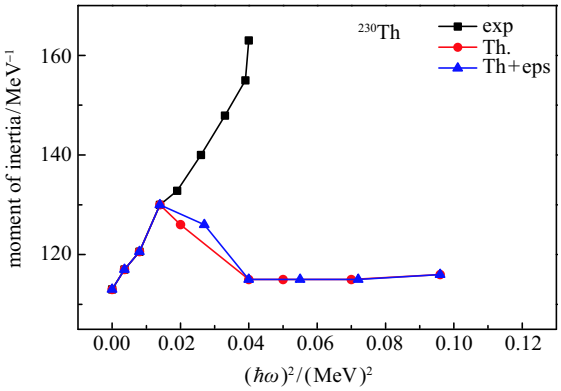

Fig. 7. (color online) The calculated moment of inertia $\frac{2\vartheta}{\hbar^2}$ versus square of rotational energy $(\hbar\omega)^2$ for ^{230}Th isotope.

3.4 Staggering in γ- band energies

The $S(J)$, particularly $S(4)$, distinguishes different model descriptions ranging from vibrational, to rotational, to axially asymmetric. It is also a useful signature of transitional regions between these ideal limiting cases

[39]. Figures 10 and 11 shows the odd–even staggering for ^{230,232,234}Th. One can see that these isotopes are deformed and no notable staggering is apparent, consistent with nuclei close to the $SU(3)$ symmetry [40].

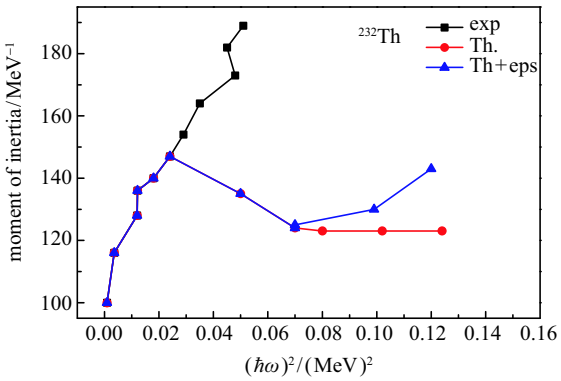

Fig. 8. (color online) The calculated moment of inertia $\frac{2\vartheta}{\hbar^2}$ versus square of rotational energy $(\hbar\omega)^2$ for ^{232}Th isotope.

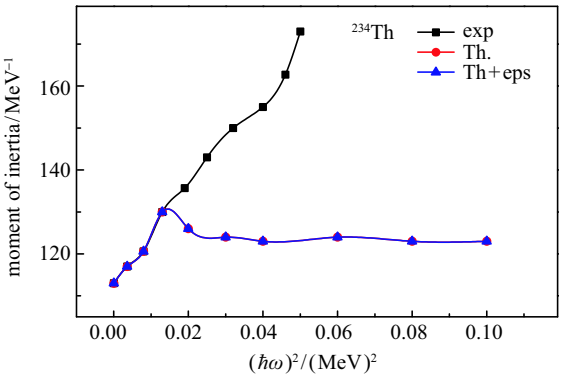

Fig. 9. (color online) The calculated moment of inertia $\frac{2\vartheta}{\hbar^2}$ versus square of rotational energy $(\hbar\omega)^2$ for ^{234}Th isotope.

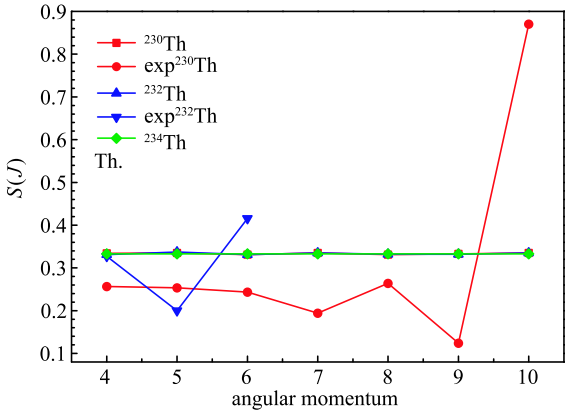

Fig. 10. (color online) Staggering $S(J)$ in γ-band calculations using Hamiltonian equation for $SU(3)$ limit and the available experimental data [42] for ^{230,232,234}Th isotopes.

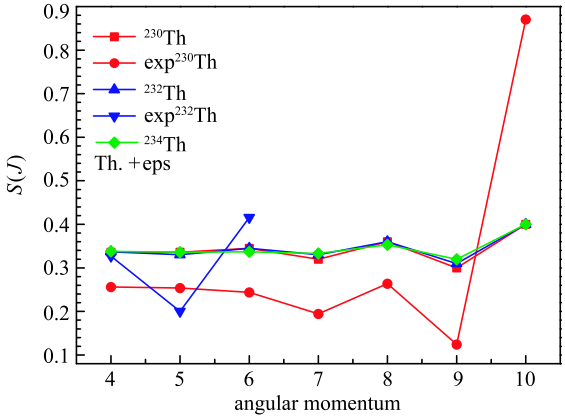

Fig. 11. (color online) Staggering $S(J)$ in γ-band calculations using Hamiltonian equation for $SU(3)$ limit +EPS and the available experimental data [42] for ^{230,232,234}Th isotopes.

3.5 Potential energy surface calculations

The potential energy surfaces were calculated to predict the lowest energy shape configurations for ^{230,232,234}Th. These are shown in Figs. 12, 13 and 14. The quadrupole deformation parameter is equivalent to $\beta > 0$ for prolate and $\beta < 0$ for oblate shapes. For γ equal to 0° [10], it is prolate type, and when γ equals 60° [19], it is oblate type [4, 23, 44]. Our main intention in this study is to obtain the first hints of nuclear phase shape in the region. In this context, we find signatures of the prolate deformation deeper than oblate, where the $\beta_{\rm min}$ of these isotopes comes equal to 1.4, for that is the $SU(3)$ limit. We can conclude that all the nuclei under study are deformed and have rotation.

4 Conclusions

The IBM-1 model has been applied to interpret the low-lying structure of the deformed nuclei ^{230,232,234}Th. From these calculations, the rotational limit has been used and the calculated results of two procedures for the predicted excited state energy levels are shown to be in agreement with the available experimental data. Absolute and relative B(E2) values were calculated and are found to be, in general, in agreement with experimental data where available. However, there is not enough experimental data in the ^{234}Th isotope for a detailed comparison and therefore, the B(E2) values and relative B(E2) were predicted for this case only.

The overlap of the wave functions for (with and without EPS) ranges from 0.98 to 1, which suggests that the ^{230,232,234}Th isotopes lie close to the $SU(3)$ limit. The square of rotational energy and the moment of inertia were reasonably produced with experimental values. The odd-even staggering in γ-bands has been studied, the $S(J)$ is weak (with and without *eps*), consistent with structures close to the $SU(3)$ limit.

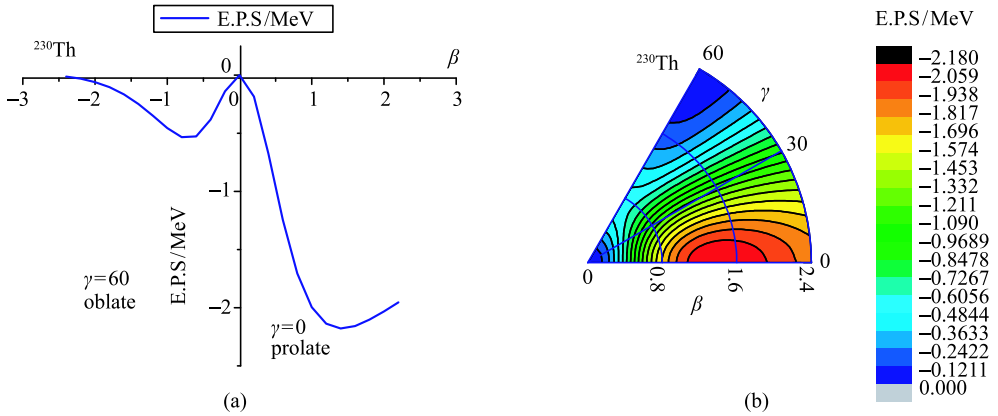

Fig. 12. (color online) (a) The potential energy surface for ^{230}Th isotope as a function of β and γ plot for γ=0 and γ=60. (b) The potential energy surface in β-γ for ^{230}Th isotope.

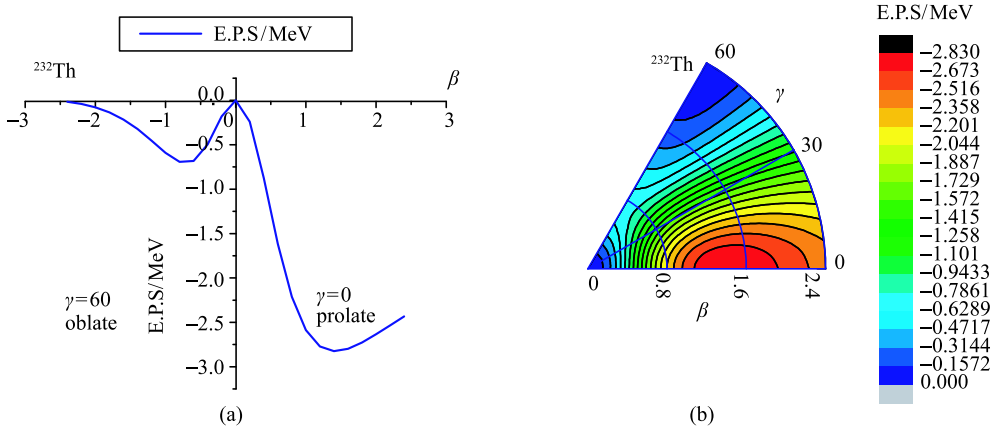

Fig. 13. (color online) (a) The potential energy surface for ^{232}Th isotope as a function of β and γ plot for γ=0 and γ=60. (b) The potential energy surface in β-γ for ^{232}Th isotope.

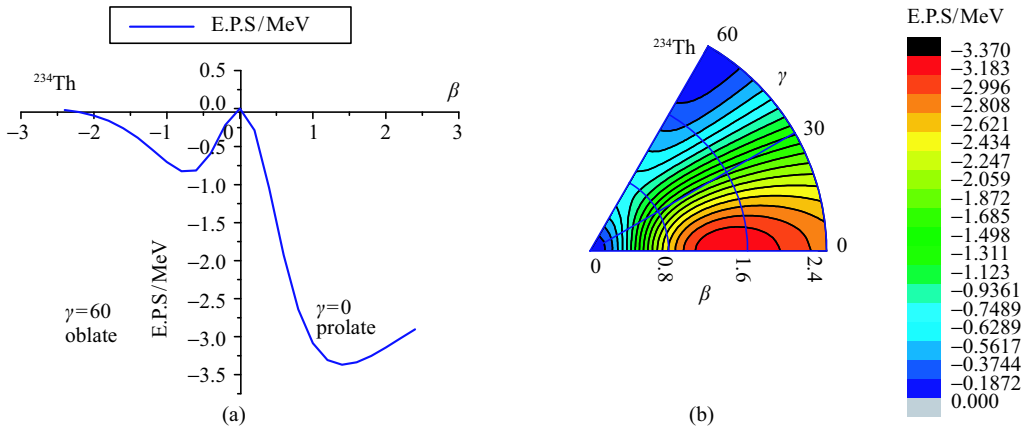

Fig. 14. (color online) (a) The potential energy surface for ^{234}Th isotope as a function of β and γ plot for γ=0 and γ=60. (b) The potential energy surface in β-γ for^{234}Th isotope.

The potential energy surfaces are calculated and predict prolate deformed states which would show clear rotational behavior for the$^{230-234}$Th isotopes.

The author wishes to acknowledge the assistance of Prof. Patrick Regan from University of Surrey (United Kingdom) for his valuable comments and discussions. Additionally, gratitude is expressed to Prof. Rich Casten

from University of Yale for his excellent comments. The author is grateful to Prof. Zsolt Podolayk from University of Surrey (United Kingdom) for his help. Finally, the invaluable support of the College of Science at the University of Kerbala is warmly acknowledged.

References

1 K. Nomura, T. Otsuka, N. Shimizu, and Lu Guo, Phys. Rev. C, **83**: 041302(R) (2011)
2 A. Bohr and B. R. Mottelson, *Nuclear Structure*, Vols. 1 and 2 (Benjamin, New York, 1969/1975)
3 P. Ring and P. Schuck, *The Nuclear Many-Body Problem* (Berlin: Springer, 1980)
4 F. Iachello and A. Arima, *The Interacting Boson Model* (Cambridge: Cambridge University Press, 1987)
5 M. S. Nadirbekov and G. A. Yuldasheva, Int. J. of Mod. Phys. E, **23**: 1450034 (2014)
6 A. Couture, R. F. Casten and R. B. Cakirli, Phys. Rev. C, **91**: 014312 (2015)
7 Ji-Wei Cui et al, Phys. Rev. C, **90**: 014321 (2014)
8 H. G. Ganev, Phys. Rev. C, **89**: 054311 (2014)
9 Bing-Nan Lu, Phys. Rev. C, **89**: 014323 (2014)
10 P. Jachimowicz, M. Kowal, and J. Skalski, Phys. Rev. C, **85**: 034305 (2012)
11 A. Frank and P. Van Isacker, *Algebraic Methods in Molecular and Nuclear Structure Physics* (New York: Wiley, 1994)
12 T. Otsuka, A. Arima, F. Iachello, and I. Talmi, Phys. Lett. B, **76**: 139 (1978); T. Otsuka, A. Arima, and F. Iachello, Nucl. Phys. A, **309**: 1 (1978)
13 T. Mizusaki and T. Otsuka, Prog. Theor. Phys. Suppl., **125**: 97 (1997)
14 K. Nomura, N. Shimizu, and T. Otsuka, Phys. Rev. Lett., **101**: 142501 (2008)
15 T. Otsuka, Phys. Lett. B, **138**: 1 (1984)
16 N. Minkov, S. B. Drenska, P. P. Raychev, R. P. Roussev, and D. Bonatsos, Phys. Rev. C, **064301**: 61 (2000)
17 D. Bonatsos, Phys. Lett. B, **200**: 1 (1988)
18 C. A. Fields, K. H. Hicks, and R. J. Peterson, Nucl. Phys. A, **431**: 473 (1984)
19 M. S. Nadirbekov and G. A. Yuldashevs. Inter. J. Mod. Phys. E, **23**: 5 (2014)
20 K. Nomura, D. Vretenar, and B.-N. Lu, Phys. Rev. C, **88**: 021303 (R) (2013)
21 Z.P. Li, B. Y. Song, J. M. Yao, D. Vretenar, and J. Meng, Phys. Lett. B, **726**: 866 (2013)
22 K. Nomura, D. Vretenar, T. Nikšiç, and B.-N. Lu, Phys. Rev. C, **89**: 024312 (2014)
23 A. Arima and F. Iachello, Ann. Phys. NY, **123**: 468 (1979)
24 A. Arima and F. Iachello, Ann. Rev. Nucl. Part. Sci., **31**: 75 (1981)
25 R. F. Casten and D. D. Warner, Rev. Mod. Phys., **60**: 391 (1988)
26 K. Kumar and M. Baranger, Nucl. Phys. A, **92**: 608 (1976)
27 R. A. Sorenson, Rev. Mod. Phys., **45**: 353 (1973)
28 R. F. Casten and D.D. Warner, Rev. Mod. Phys., **60**: 389 (1988)
29 A. Arima and F. Iachello, *The Interacting Boson Model* (Cambridge: Cambridge University press, 1987)
30 E. A. McCutchan and N. V. Zamfir, Phys. Rev. C, **71**: 054306 (2005)
31 H. H.Kassim and F. I. Sharrad, Int. J. Mod. Phys. E, **23**(11): 1450070 (2014)
32 K. S. Karne and R. M. Steffen, Phys. Rev. C, **2**: 724 (1970)
33 F. I. Sharrad, H. Y. Abdullah, N. Al-Dahan, N. M. Umran, A. A. Okhunov, and H. A. Kassim , Chin. Phys. C, **37**: 034101 (2013)
34 A. A. Okhunov, F. I. Sharrad, Anwer A. Al-Sammarraie, and M. U. Khandaker, Chin Phys. C, **39**: 084101 (2015)
35 J. E. Garcia and K. Heyde, Nucl. Phys. A, **825**: 39 (2009)
36 K. S. Krane, *Introductory Nuclear Physics* (New York: Johen Wiley and Sons, 1988)
37 R. F. Casten and D. D. Warner, *Algebraic Approaches to Nuclear Structure. Interacting Boson and Fermion Models* (USA: Harwood academic publishers, 1993)
38 V. Devi, Turk. J. Phys., **37**: 330 (2013)
39 R. F. Casten, *Nuclear Structure from a Simple Perspective* (New York: Oxford Science Publication, 2000)
40 R. F. Casten et al, Phys. Rev. C, **76**: 024306 (2007)
41 O. Scholten, *Computer code PHINT, KVI* (Holland: Groningen, 1980)
42 http://www.nndc.bnl.gov/chart/ Online database, National Nuclear Data Centre (Site Visited: August, 2015)
43 L. M. Robledo el al, Phys. Rev. C, **77**: 064322 (2009)
44 D. Bonatsos, *Interacting Boson Models of Nuclear Structure* (Ed. David, Stanford, New York: Oxford University Press, 1988)